PAST AND FUTURE SEA SURFACE TEMPERATURE CHANGES IN THE OCEANS SURROUNDING CANADA

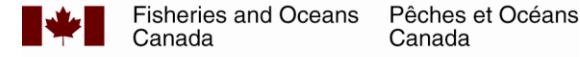
Zeliang Wang¹, Blair J.W. Greenan¹, Charles G. Hannah², and Chantelle Layton¹

¹Bedford Institute of Oceanography 1 Challenger Drive Dartmouth, Nova Scotia Canada B2Y 4A2

²Institute of Ocean Sciences 9860 West Saanich Road Sidney, BC Canada V8L 4B2

2025

Canadian Technical Report of Hydrography and Ocean Sciences 404





Canadian Technical Report of Hydrography and Ocean Sciences

Technical reports contain scientific and technical information of a type that represents a contribution to existing knowledge but which is not normally found in the primary literature. The subject matter is generally related to programs and interests of the Oceans and Science sectors of Fisheries and Oceans Canada.

Technical reports may be cited as full publications. The correct citation appears above the abstract of each report. Each report is abstracted in the data base *Aquatic Sciences and Fisheries Abstracts*.

Technical reports are produced regionally but are numbered nationally. Requests for individual reports will be filled by the issuing establishment listed on the front cover and title page.

Regional and headquarters establishments of Ocean Science and Surveys ceased publication of their various report series as of December 1981. A complete listing of these publications and the last number issued under each title are published in the *Canadian Journal of Fisheries and Aquatic Sciences*, Volume 38: Index to Publications 1981. The current series began with Report Number 1 in January 1982.

Rapport technique canadien sur l'hydrographie et les sciences océaniques

Les rapports techniques contiennent des renseignements scientifiques et techniques qui constituent une contribution aux connaissances actuelles mais que l'on ne trouve pas normalement dans les revues scientifiques. Le sujet est généralement rattaché aux programmes et intérêts des secteurs des Océans et des Sciences de Pêches et Océans Canada.

Les rapports techniques peuvent être cités comme des publications à part entière. Le titre exact figure au-dessus du résumé de chaque rapport. Les rapports techniques sont résumés dans la base de données *Résumés des sciences aquatiques et halieutiques*.

Les rapports techniques sont produits à l'échelon régional, mais numérotés à l'échelon national. Les demandes de rapports seront satisfaites par l'établissement auteur dont le nom figure sur la couverture et la page de titre.

Les établissements de l'ancien secteur des Sciences et Levés océaniques dans les régions et à l'administration centrale ont cessé de publier leurs diverses séries de rapports en décembre 1981. Vous trouverez dans l'index des publications du volume 38 du *Journal canadien des sciences halieutiques et aquatiques*, la liste de ces publications ainsi que le dernier numéro paru dans chaque catégorie. La nouvelle série a commencé avec la publication du rapport numéro 1 en janvier 1982.

Canadian Technical Report of Hydrography and Ocean Sciences 404

2025

Past and future sea surface temperature changes in the oceans surrounding Canada

by

Zeliang Wang¹, Blair J.W. Greenan¹, Charles G. Hannah², and Chantelle Layton¹

¹Science Branch, Maritimes Region Bedford Institute of Oceanography Fisheries and Oceans Canada 1 Challenger Drive Dartmouth, Nova Scotia Canada B2Y 4A2

> ²Science Branch, Pacific Region Institute of Ocean Sciences Fisheries and Oceans Canada 9860 West Saanich Road Sidney, BC Canada V8L 4B2

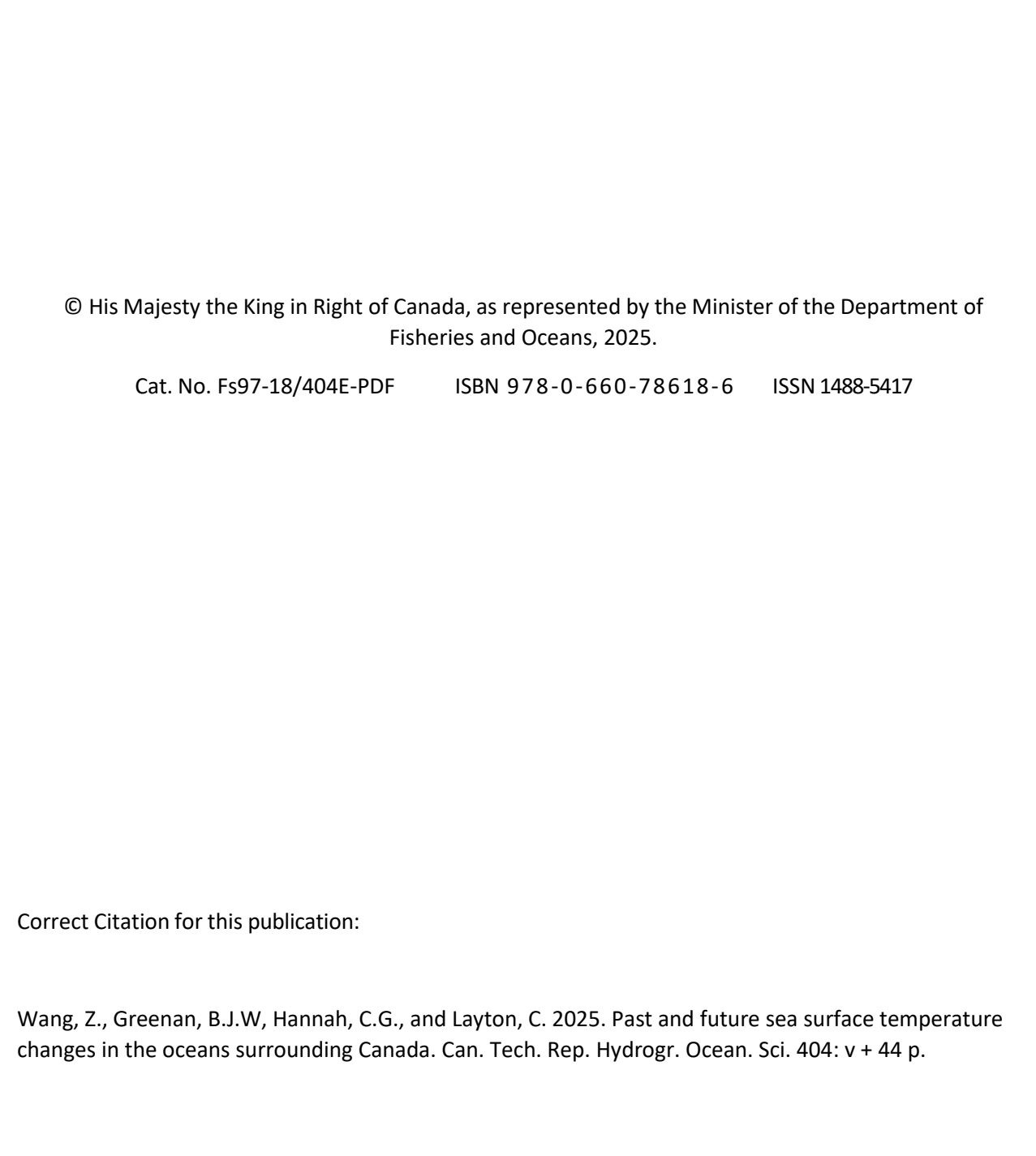


TABLE OF CONTENTS

ABSTRACT	v
RÉSUMÉ	vi
1. Introduction	1
2. Datasets and methodology	4
2.1 Hadley Centre Sea Ice and Sea Surface Temperature (HadISST)	4
2.2 Coupled Model Intercomparison Project Phase 6 (CMIP6)	5
2.3 In situ temperature observations	6
2.4 Methodology	7
3. Results	9
3.1 SST variability	9
3.2 Historical SST changes	16
3.3 Projected SST changes	19
4. Discussion and conclusion	24
Acknowledgements	29
References	30
Appendix	40

ABSTRACT

Wang, Z., Greenan, B.J.W., Hannah, C.G., and Layton, C. 2025. Past and future sea surface temperature changes in the oceans surrounding Canada. Can. Tech. Rep. Hydrogr. Ocean. Sci. 404: v + 44 p.

This study presents changes in the sea surface temperature (SST) in the oceans surrounding Canada using past observations and model projections of future scenarios. The past changes are derived using an SST product, HadISST, in which a recent period (2012-2022) was referenced to a 26-year climatology (1955-1980). The future changes in SST are estimated using a 22-member ensemble of CMIP6 models. The SST changes for overlapping periods from the CMIP6 ensemble and the HadISST in the 10 regions of the Canadian shelf waters are in general agreement, although the CMIP6 results tend to overestimate the observed changes by about 0.1 °C. One exception to this is the Scotian Shelf where the CMIP6 models underestimate the observed SST change. The Gulf of Maine, Scotian Shelf, Gulf of St. Lawrence and southern Newfoundland shelf are the regions with the largest observed SST increases around Canada. The Gulf of St. Lawrence has the highest correlation (r=0.65) with the Atlantic Multi-decadal Oscillation (AMO) among the subregions in the North Atlantic Ocean, and the British Columbia Shelf is correlated with the Pacific Decadal Oscillation (r=0.58). Under the four climate scenarios (SSP1-2.6 to SSP5-8.5), among the mid-century (2040-2059) annual mean SST changes (reference period of 1990-2014) in the 10 regions, the Gulf of St. Lawrence is projected to have the largest increases in temperature $(1.8 - 2.5^{\circ}\text{C})$, and Baffin Bay has the smallest increases (0.5 – 0.9°C), However, for the summer means, the southern Beaufort Sea has the largest SST increase (2.4 -3.1°C) with Baffin Bay having the smallest changes (1.3-2.1°C).

RÉSUMÉ

Wang, Z., Greenan, B.J.W., Hannah, C.G., and Layton, C. 2025. Past and future sea surface temperature changes in the oceans surrounding Canada. Can. Tech. Rep. Hydrogr. Ocean. Sci. 404: v + 44 p.

Cette étude présente les changements de la température de la surface de la mer (TSM) dans les océans entourant le Canada en s'appuyant sur les observations antérieures et sur des projections modélisées de scénarios futurs. Les changements antérieurs sont obtenus à l'aide d'un produit de TSM, le HadISST, dans lequel une période récente (2012 à 2022) a été référencée à des données climatologiques sur 26 ans (1955 à 1980). Les changements futurs de la TSM sont estimés au moyen d'un ensemble de 22 membres de modèles du CMIP6. Les changements de la TSM pour les périodes de chevauchement de l'ensemble du CMIP6 et du HadISST dans les 10 régions des eaux du plateau canadien concordent généralement, bien que les résultats du CMIP6 tendent à surestimer les changements observés d'environ 0,1 °C. Une exception à cette observation est le plateau néo-écossais, où les modèles du CMIP6 sous-estiment le changement de la TSM. Le golfe du Maine, le plateau néo-écossais, le golfe du Saint-Laurent et le sud du plateau de Terre-Neuve sont les régions où la TSM a augmenté le plus au Canada. Le golfe du Saint-Laurent présente la plus forte corrélation (r = 0,65) avec l'oscillation multidécennale de l'Atlantique parmi les sous-régions de l'océan Atlantique Nord, et le plateau de la Colombie-Britannique est corrélé avec l'oscillation décennale du Pacifique (r = 0,58). Selon les quatre scénarios climatiques (SSP1-2.6 à SSP5-8.5), parmi les variations annuelles moyennes de la TSM au milieu du siècle (2040 à 2059; période de référence de 1990 à 2014) dans les 10 régions, c'est le golfe du Saint-Laurent qui devrait connaître les plus fortes augmentations de température (1,8 à 2,5 °C), tandis que la baie de Baffin montre les plus faibles augmentations (0,5 à 0,9 °C). Toutefois, en ce qui concerne les moyennes estivales, le sud de la mer de Beaufort connaîtrait la plus forte augmentation de la TSM (2,4 à 3,1 °C), alors que les plus faibles changements seraient observés dans la baie de Baffin (1,3 à 2,1 °C).

1. Introduction

As the country with the longest coastline in the world, surrounded by three oceans (the North Atlantic, Arctic and North Pacific), Canada is strongly influenced by changes in the oceans and the adjacent Canadian shelf waters (CSW, hereafter), which lie above the relatively shallow continental shelves. The CSW encompass a vast and dynamic marine environment, characterized by a complex interplay of oceanic currents, atmospheric conditions, and geographic features (e.g., Loder et al., 1998; Wang et al., 2015; Brickman et al., 2018; Han et al., 2019). Among the crucial factors shaping this system, temperature stands out as a fundamental driver influencing biological processes and ecological dynamics (e.g., Beazley et al., 2018; Shackell et al., 2019; Wang et al., 2020a; Wang et al., 2020b; Lehmann et al., 2023; Cyr et al., 2024; Marsh et al., 1999). Understanding the temporal variability and changes of temperatures in these shelf waters is essential for unraveling ecosystem dynamics, assessing climate change impacts, and informing sustainable management practices.

The CSW exhibit remarkable diversity in temperature regimes with very cold Arctic waters in the northern areas to warmer SST in southern Atlantic Canada and the waters adjacent to British Columbia (Larouche and Galbraith, 2016). This diversity is influenced by a multitude of factors, including latitude, coastal proximity, upwelling events, freshwater input from rivers, and interactions with major ocean currents such as the Labrador Current (e.g., Wang et al., 2016), the Gulf Stream (e.g., Wang et al., 2022), and the California Current system (e.g., Checkley and Barth, 2009). Seasonal and interannual variability strongly influences the temperature landscape. In addition to the diversity in the temperature environment, CSW regions are also characterized by strong biodiversity of their ecosystems and serve as critical habitats for numerous species of fish, invertebrates, marine mammals, and seabirds (Le Corre et al., 2020; Kenchington et al., 2019; Stanley et al., 2018). The shallow depths and nutrient-rich waters of

the shelves foster the growth of phytoplankton and other primary producers, forming a strong base for food webs. This rich biodiversity not only supports commercial fisheries but also contributes to the overall health and resilience of marine ecosystems.

Knowledge of the historical (observed) and future (projected) temperature changes has the potential to improve our understanding of changes that have occurred in ocean ecosystems and to plan for future changes expected as a result of climate change. There are numerous studies which have demonstrated that climate change can have significant impacts on the ecosystems of the CSW (e.g., O'Brien et al., 2022, Greenan et al., 2019, Baye et al., 2019, Lowen et al., 2017, Beazley et al., 2021., Lyons et al., 2019, Pratt et al., 2022, Okey et al., 2014, Wassmann, et al., 2011).

Observations-based SST products provide a resource for investigating sea surface temperature (SST) variability and change since the 1950s. While there is SST data available prior to the mid-20th century, the data are sparse and less reliable in the waters surrounding Canada. Several high-quality SST products are publicly available, such as HadlSST (Rayner et al., 2003), ERSST (Smith et al., 2008), OISST (Huang et al., 2021), and COBE (Ishii et al., 2005). Although the methodologies for producing these gridded products vary and their resolutions differ, Loder and Wang (2015) demonstrated that these products tend to have similar accuracy in representing observed SST.

The Coupled Model Inter-comparison Project (CMIP; Meehl et al., 2007; Taylor et al., 2012) is a core element of national and international assessments of climate change. CMIP6 is the latest modeling effort for simulating and projecting various aspects of climate change for which a new set of scenarios has been developed. CMIP5 uses Representative Concentration Pathways (RCPs) to represent greenhouse gas concentration trajectory. In contrast, the new scenarios in CMIP6 represent different socio-economic scenarios as well as different pathways of atmospheric greenhouse gas concentrations

(Shared Socio-economic Pathways; SSPs; from SSP1 to SSP5). The projections from this latest modelling efforts provide an invaluable opportunity to investigate the range of potential scenarios for the future SST in the CSW (e.g., Wang et al., 2024).

Many previous studies (e.g., Loder et al., 2015; Wang et al., 2024) have demonstrated that solutions from the CMIP6 models have a large spread, mainly due to large variations in climate from internal variability in the climate system (Stevenson et al., 2023). An ensemble approach is the most common methodology applied in the analysis and use of the CMIP6 solutions, e.g., Loder et al., 2015; Wang et al., 2024; Ren et al., 2024. For the purpose of this work, the ensemble approach for the analysis of CMIP6 SST means combining the SSTs from multiple CMIP6 models to produce a more robust and reliable prediction of future SST changes, by calculating a mean value across all the models, effectively reducing the uncertainties associated with any single model's simulation.

CMIP6 models are inherently coarse in spatial resolution due to their global scale (Wang et al., 2024). The question of whether these coarse resolution models can capture variations of ocean conditions in the shallow shelf waters is a reasonable concern. On global scales, Zhang et al. (2023) reported that, CMIP6 models perform better than CMIP5 ones in reproducing SST climatology, with a lower multi-model ensemble mean of globally averaged absolute bias. Wang et al. (2024] demonstrated that ensemble means of the CMIP6 models do have the ability to represent SST on the Scotian Shelf with relative accuracy. Pereira et al.(2024) demonstrated that CMIP6 models reproduced the historical patterns of meteo-oceanographic properties for the Spanish continental coasts. Purich and England (2021) assessed Antarctic Shelf Bottom Water (ASBW) temperature mean-state and trends in CMIP6 models, and concluded that CMIP6 ensemble mean zonal temperature structure and mean-state ASBW spatial pattern were close to the observed patterns, while despite considerable spread across the CMIP6 models. These previous studies indicate that the CMIP6 models can be used to investigate

oceanographic changes in the shelf waters, which underscores the potential usages of the CMIP6 results for the CSW.

This study will use the SST product HadISST, and CMIP6 model solutions to investigate past and future SST changes in the CSW. Performance of the ensemble means of the 22 CMIP6 model solutions for the CSW is investigated as well. Section 2 provides the details of datasets used in this study, as well as the methodology. The results are reported in Section 3, and the discussion about the findings and the conclusion of this study are presented in Section 4.

2. Datasets and methodology

2.1 Hadley Centre Sea Ice and Sea Surface Temperature (HadISST)

The HadISST dataset is a widely-used gridded dataset that provides historical records of sea surface temperatures (SST) and sea ice concentrations (Rayner et al., 2003). HadISST covers the period from 1870 to the present, offering a long-term perspective on oceanic conditions. It is a valuable resource for understanding historical and ongoing changes in sea surface temperatures and sea ice extent at a global scale. HadISST combines observations from various sources including ships, buoys, and satellites, along with statistical methods for spatial interpolation, to create global coverage of SST and sea ice data. HadISST provides monthly SST for the entire globe, including oceanic and sea ice regions, with a grid resolution of 1° latitude by 1° longitude. In regions of the ocean that are covered permanently by seasonal sea ice, the SST in the HadISST product is set to a value of -1.8°C.

2.2 Coupled Model Intercomparison Project Phase 6 (CMIP6)

The Coupled Model Intercomparison Project Phase 6 (CMIP6) represents the latest generation of climate models developed by the global scientific community (Eyring et al., 2016). These models are designed to simulate Earth's climate system and its various components, including the atmosphere, oceans, land surface, and cryosphere. CMIP6 builds upon previous iterations and provides enhanced capabilities and improved representations of key processes. The simulations of the CMIP6 models have two temporal segments: the first one is the historical period which ends in 2014, and the second is the simulations after 2014 for climate projections. This study focuses on the data from the historical and future period of 1955-2059, however, analysis for the late 21st century (2080-2099) is also presented in the Appendix of this report.

CMIP6 model results encompass a wide range of variables and scenarios, allowing researchers to explore different aspects of past, present, and future climate conditions. These results include simulations of historical climate conditions and projections of future climate change under various greenhouse gas emission scenarios. CMIP5 uses Representative Concentration Pathway (RCP) to represent a greenhouse gas concentration trajectory. In contrast, the new scenarios in CMIP6 represent different socio-economic developments as well as different pathways of atmospheric greenhouse gas concentrations (Shared Socio-economic Pathways; SSPs; from SSP1 to SSP5). In this study, we focus on SSP1-2.6, SSP2-4.5, SSP3-7.0 and SSP5-8.5. The number at the end of each scenario name represents the level of additional radiative forcing in watts per square meter by the year 2100.

It is widely recognized in the climate science community that no single CMIP model is able to provide a robust representation of all of the important processes in the climate system, especially those affecting regional climate (Loder et al., 2015, and references therein). IPCC projections are based on the statistics of an ensemble of models. A similar approach is also needed to represent regional climate and,

in this study, the ensemble mean of 22 CMIP6 models is used. Some details of these models can be found in Wang et al. (2024).

2.3 In situ temperature observations

Fisheries and Oceans Canada (DFO) Atlantic Zone Monitoring Program (AZMP) has a number of sites with regularly scheduled monitoring of physical, biological, and chemical oceanographic conditions. In the DFO Maritimes region, there are two sites, Prince 5 (P5) and Station 2(S2). Prince 5 (66.850 ° W, 44.90 ° N) is located near the entrance of the Bay of Fundy and is used as a proxy to describe environmental conditions in the Bay of Fundy. This station has been sampled since 1924 and is sampled once a month. Station 2 on the Halifax Line, often referred to as S2, is located approximately ten nautical miles outside of Halifax Harbor (63.317° W, 44.267° N), and is representative of the broader conditions on the Scotian Shelf. The station has been sampled approximately twice monthly since the inception of the Atlantic Zone Monitoring Program (AZMP) in 1999. The time series from Station 2 is extended to the period before AZMP using data acquired near the location prior to the program. The near surface temperature data presented in this report for Prince 5 and Station 2 are derived from a layer of 0-5 m depth. In the DFO Newfoundland Region, Station 27 (52.587 °W, 47.547° N; S27) is located in the Avalon Channel outside of St. John's Harbour. It is one of longest hydrographic time series in Canada with frequent (near-monthly basis) conductivity-temperature-depth (CTD) observations since 1946. Station 27 was integrated into DFO's AZMP in 1999 (Cyr and Galbraith, 2021). Due to limitations of this data set, temperature data presented in this study are integrated over the whole water column depth of 0 to 176 m and, therefore, does not represent the surface layer alone.

For the waters adjacent to the west coast of Canada, DFO has a long-term monitoring program for ocean surface temperature entitled the <u>British Columbia Shore Station Oceanographic Program</u> (BCSS). This coastal time series (representative of near-surface regional average shelf waters; the average of the station across the BC coast) collected at lighthouse stations dating back to 1914 (Donnet et al., 2023). In Canadian Pacific waters, the coastal SST variability has been shown to be strongly influenced by large-scale climate processes and by local wind forcing (Cummins & Masson, 2014).

2.4 Methodology

This study aims to explore changes in SST both historically and in future projections within the Canadian shelf waters. SST variations spanning from 1950 to 2022 are examined at a range of spatial scales including the global ocean, the North Atlantic Ocean, the North Pacific Ocean, and for defined area of the Canadian shelf waters. To represent past climatology, a 26-year period from 1955 to 1980 is derived from the HadISST dataset. The period of 2012-2022 is treated as the present state of the SST, and the SST change between the last decade and the 26-year climatology is investigated.

Given that the historical simulations of CMIP6 models conclude in 2014, projections for the future period of 2040-2059 are compared to a historic reference period of 1990-2014 to analyze SST projections. The choice of the historical reference period is supported by several studies (Wang et al. 2015, 2016, 2019), which have documented substantial changes in temperature in the North Atlantic Ocean during the early 1990s. Recognizing the potential influence of these changes on decadal or even longer-term oceanic variability, we have selected 1990-2014 as our climatological period.

For this study, 10 regions of the Canadian shelf waters are defined to provide an area average estimate of SST change (Table 1). While the Canadian Arctic Archipelago remains mostly ice-covered and

thus excluded from investigation, the southern Beaufort Sea is included due to its ice-free summer season. Defining the outer limit of the shelf waters poses challenges due to significant variations in the shelf-break slope. To address this, we employed both traditional and simplified approaches while considering the complexities of local benthic features. The outer limit is delineated at the 200 m isobath for the Gulf of Maine and Scotian Shelf, 400 m for the Newfoundland and Labrador shelves, and 600 m for the Arctic and Pacific regions. It's noteworthy that the entire Hudson Bay and Baffin Bay were included in the analysis for simplicity, with only the western part of Baffin Bay in Canada's Exclusive Economic Zone, and only the northern part of the Gulf of Maine falling within Canadian jurisdiction.

Table 1. The polygon IDs, abbreviations and names of the 10 shelf regions

Polygon ID	Abbreviations	Names of the regions
1	GoM	Gulf of Maine
2	SS	Scotian Shelf
3	GSL	Gulf of St. Lawrence
4	SNS	Southern Newfoundland Shelf
5	NNS	Northern Newfoundland Shelf
6	LS	Labrador Shelf
7	НВ	Hudson Bay
8	ВВ	Baffin Bay
9	BCS	British Columbia Shelf
10	SBS	Southern Beaufort Sea

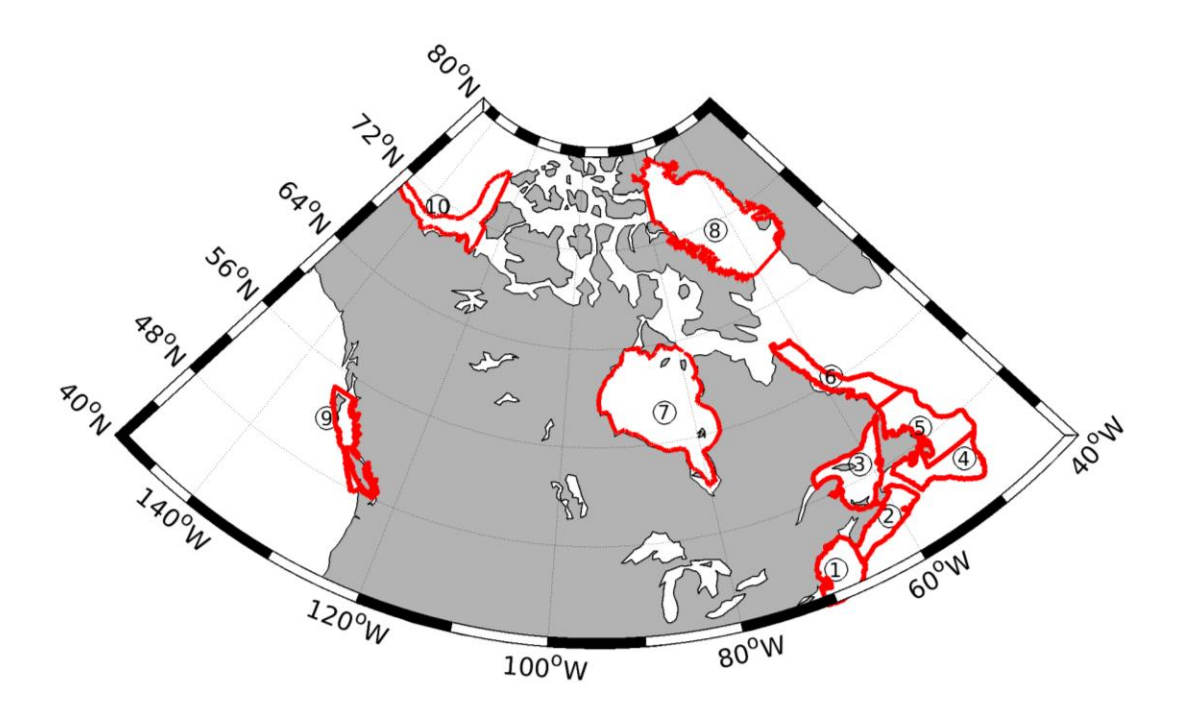


Figure 0: The location of each region in Table 1

3. Results

3.1 SST variability

SST in the oceans surrounding Canada, and at the global scale, exhibits different levels of seasonal and long-term variability driven by external factors as well as internal dynamics. At a national level, it is important to assess and compare the SST variability in the CSW regions defined in Table 1. As a first step, annual mean SST anomalies for the global oceans (between 60°S to 60°N, tropical, subtropical and subpolar), North Atlantic (30°N to 60°N/100.5°W to 29.5°E, subtropical and subpolar), and North Pacific (30°N to 60°N/105.5°E to 105.5°W, subtropical and subpolar) are shown in Figure 1. This demonstrates that individual ocean basins display stronger inter-annual variability compared to the global average, and indicates that there are significant spatial variation in SST distribution. From 1950 to 2022, the mean SST of the global oceans exhibits a consistent warming trend, albeit interrupted by a hiatus lasting approximately a decade during the 2000s. However, both the North Atlantic and North

Pacific regions exhibit clear multi-decadal variations. In the North Atlantic, a cooling trend prevailed from the early 1950s until the early 1970s, followed by a warming trend. Conversely, in the North Pacific, the cooling trend commenced later, around the mid-1960s, persisting until the mid-1970s, after which a warming trend emerged. Despite having similar long-term warming trends, the North Atlantic and North Pacific oceans display distinct interannual variabilities.

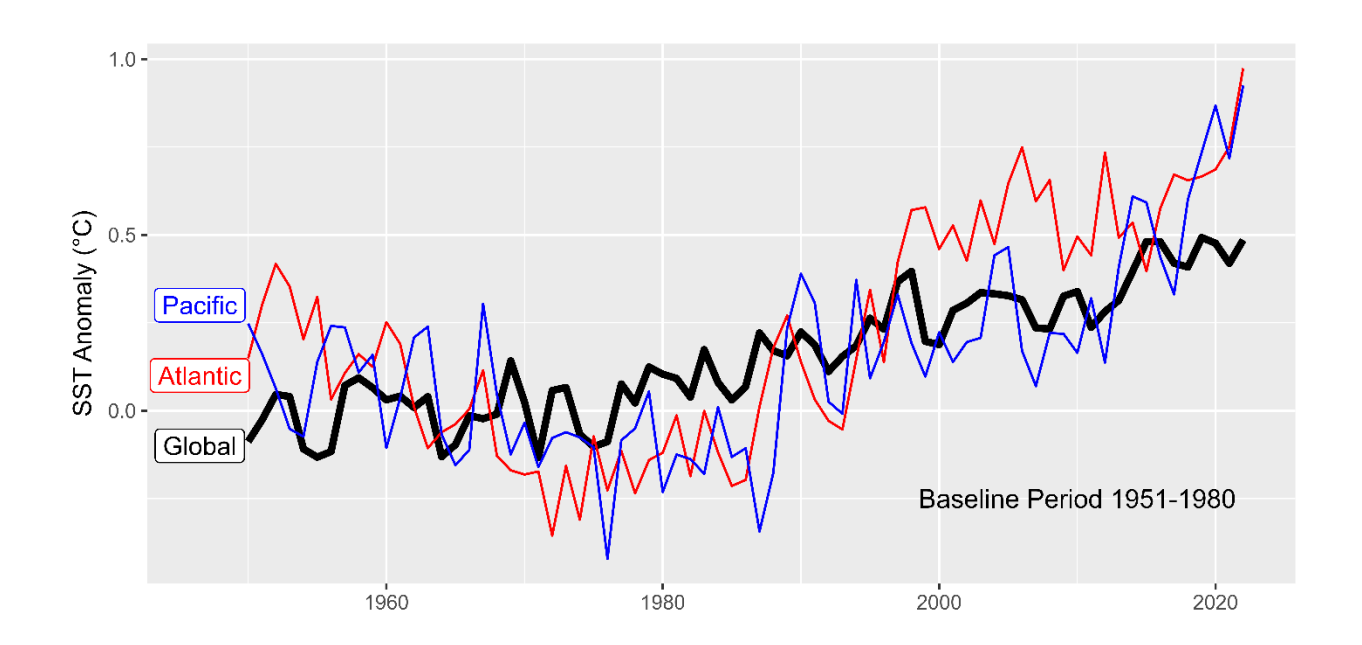


Figure 1: Annual-average sea surface temperature anomalies for the global, North Atlantic and North Pacific oceans. The reference period for the computation of the anomalies is 1951-1980.

To assess whether the SST variations observed in the North Atlantic and North Pacific Oceans are mirrored in the 10 regions of the CSW, SST anomalies across these regions from 1950 to 2022 are presented in Figure 2. The majority of these 10 regions exhibit larger ranges of anomalous SST compared not only to the global oceans but also to both the North Atlantic and North Pacific regions (as illustrated in Figure 1). Notably, the GoM and SS show the largest ranges of 4.0°C, highlighting substantial SST variability within the CSW. The BB displays the smallest range of anomalies at 1.1°C.. Figure 2 underscores the significant SST variability within the CSW.

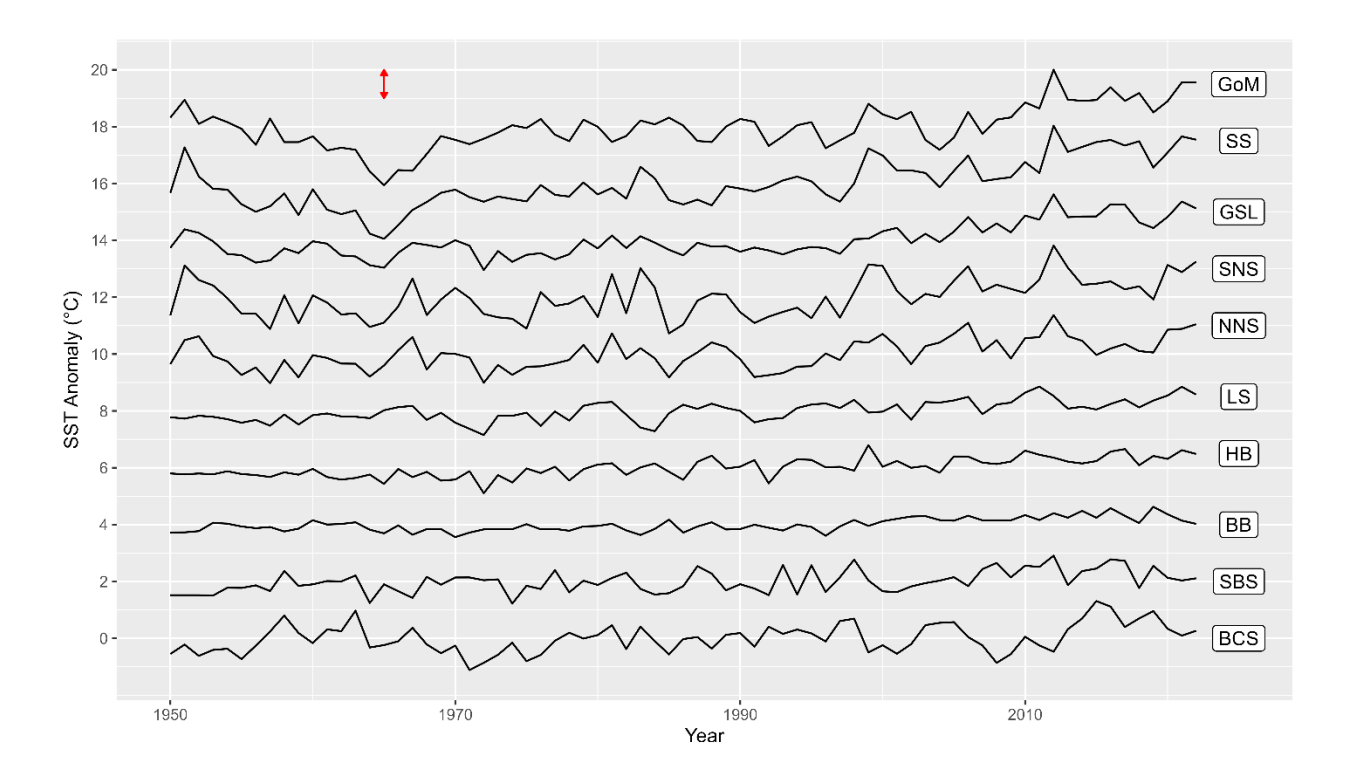


Figure 2: Annual average sea surface temperature anomalies for each of the 10 CSW regions of the CSW as defined in Table 1. The reference period for the anomalies is 1951-1980. The time series are each offset by 2°C for clarity. The red scale arrow represents a change of 1°C.

The SST anomalies averaged over the whole North Atlantic Ocean during the early 1970s (Figure 1) do not correlate with patterns observed within the regional CSW. Instead, minima during the mid-1960s are evident in the GoM, SS, and marginally in the GSL. Small negative anomalies during the mid-1970s and mid-1960s are observed in the SNS and NNS, respectively, with their minima appearing in the late 1950s. Regions like LS, HB, and BB display minimal variability before 1970, with this trend persisting through the period, although stronger variations emerge in recent years. This suggests that the presence of ice cover in these regions strongly limits their SST variability. The pronounced spatial variations of SST in the North Atlantic Ocean likely contribute to the divergent timings of minima between the ocean and its shelf waters. Continued warming trends are evident after the mid-1960s in the GoM, SS, and GSL,

with similar trends observed in SNS and NNS, although with a hiatus between 1970 and 1990 before resuming after 1990. The LS, HB, and BB exhibit a general slight warming trend throughout the period, interspersed with occasional short cooling periods.

In the BCS, the minimum occurred in 1971, several years prior to the mid-1970s minimum in the North Pacific Ocean (Figure 1). A clear warming trend is not apparent throughout the entire period in the BCS, and although there has been an increase in the most recent decade this was strongly influenced by the marine heat wave in the Pacific in 2014-15. In the SBS, two minima occur, one in the mid-1960s and another in the mid-1970s, with a slight warming trend observed throughout the period.

To quantitatively assess the potential connection between SST variations in the 10 regions and the broader oceans they are a part of, correlation coefficients were calculated. Two sets of calculations were performed: one using the original (non-detrended) data from Figures 1 and 2, and the other using detrended data. The correlation coefficients are presented in Table 2. Note that the BB and HB regions used the timeseries for the North Atlantic Ocean, and since we don't have timeseries for the Arctic Ocean, data for both the North Atlantic Ocean and North Pacific Ocean were used in SBS (P for North Pacific and A for North Atlantic in Table 2).

Table 2. Correlation coefficients(r) between SST in the 10 regions and the oceans they belong to (the underlined numbers are the correlations with p values > 0.05)

	GoM	SS	GSL	SNS	NNS	LS	НВ	BB	BCS	SBS/P	SBS/A
Non-detrended	0.58	0.71	0.78	0.64	0.69	0.64	0.69	0.68	0.52	0.2	0.36
Detrended	0.33	0.46	0.59	0.50	0.53	0.37	0.42	0.43	0.41	<u>-0.13</u>	0.06

It's evident that the data that are not detrended consistently yield higher correlations compared to the detrended data, indicating that the higher correlations in the non-detrended data stem from trends present in both the CSW regions and the two ocean basins. Notably, the Southern Beaufort Sea

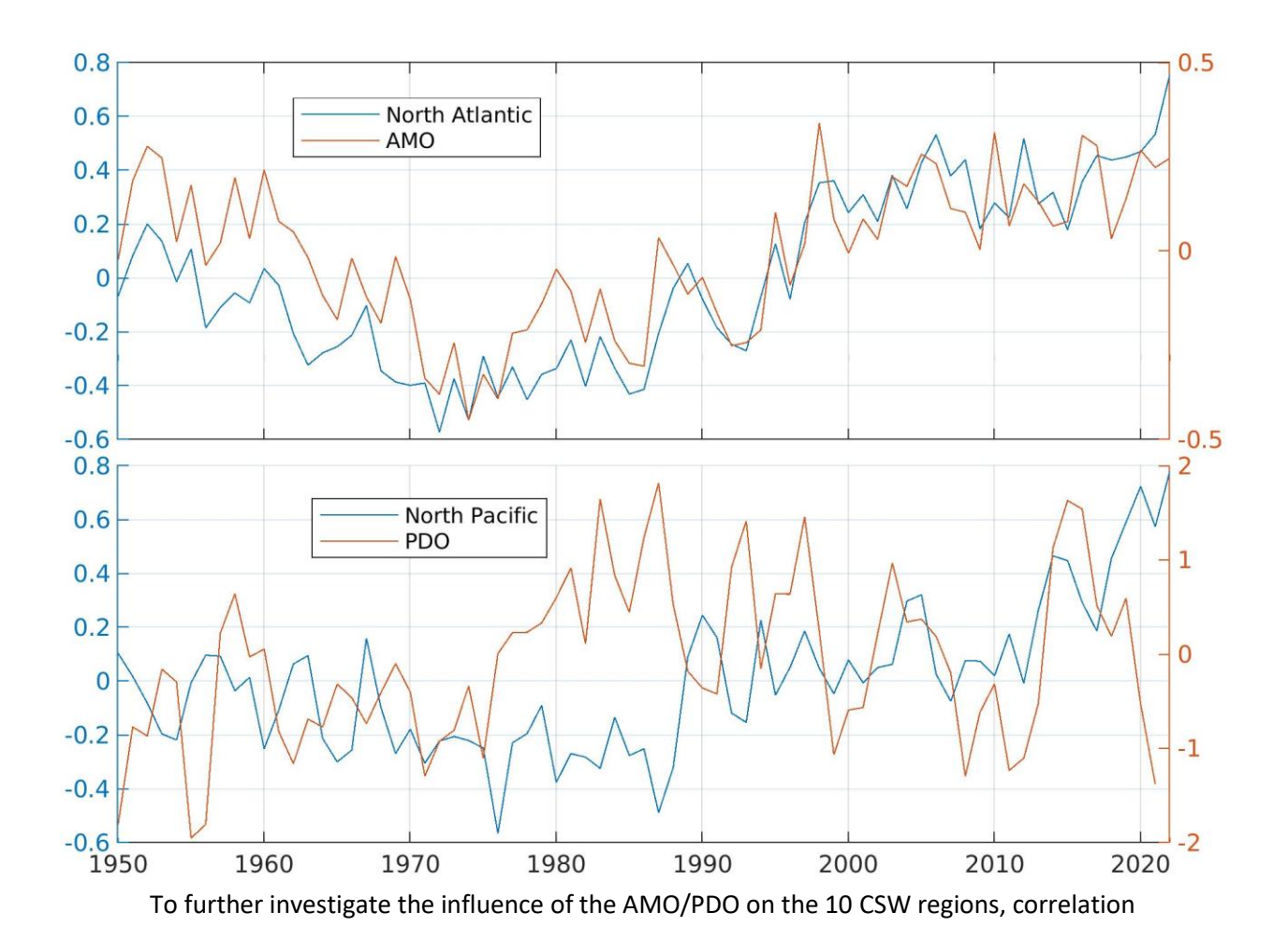
(SBS) exhibits a higher correlation with the North Atlantic Ocean than with the North Pacific Ocean in the non-detrended data In the North Atlantic Ocean regions, correlations from the non-detrended data are generally above 0.64, except for the GoM at 0.58. Among them, the GSL displays the highest correlation of 0.78, followed by the SS at 0.71. Conversely, the correlations for the BCS are low (0.52 for non-detrended and 0.41 for detrended data), suggesting that this region does not closely correspond to the general changes in the entire North Pacific Ocean.

The Atlantic Multi-decadal Oscillation (AMO; https://psl.noaa.gov/data/climateindices) and Pacific Decadal Oscillation (PDO; https://psl.noaa.gov/data/climateindices) serve as indices reflecting long-term variations in SST for the North Atlantic Ocean and North Pacific Ocean, respectively. We examined the relationship between these indices and their corresponding oceans (Figure 3). The correlation coefficient between the AMO and the SST of the defined North Atlantic Ocean in this study is 0.84 (p<0.001), whereas no statistically significant correlation is found between the PDO and the SST of the defined North Pacific Ocean. The AMO pattern predominantly exhibits a positive trend across the entire North Atlantic Ocean (https://en.wikipedia.org/wiki/Atlantic_multidecadal_oscillation), while the PDO is the dominant mode of SST variability in the North Pacific and is characterized by higher

temperatures in the west and lower temperatures in the east, or vice versa.

(https://en.wikipedia.org/wiki/Pacific decadal oscillation).

Figure 3. Timeseries of the SST for North Atlantic Ocean and AMO (top panel) and those of the SST for the North Pacific Ocean and PDO (bottom panel).



coefficients between the AMO/PDO and SST in each region were calculated following the approach used in Table 2, and are listed in Table 3. For the 8 regions in the North Atlantic Ocean, correlations with non-detrended data are generally smaller than those listed in Table 2. The BCS displays a stronger correlation with the PDO compared to the SST from the defined North Pacific Ocean in this study, for both non-

detrended and detrended data. Similarly, the SBS exhibits stronger correlations with both AMO and PDO compared to the SST from the defined oceans in this study, for both non-detrended and detrended data.

Table 3. Correlation coefficients between the SST in 10 regions and the AMO or PDO

	GoM	SS	GSL	SNS	NNS	LS	НВ	ВВ	BCS	SBS/P	SBS/A
Non-detrended	0.40	0.51	0.65	0.54	0.61	0.53	0.52	0.58	0.59	0.22	0.38
Detrended	0.27	0.41	0.63	0.46	0.53	0.45	0.43	0.51	0.54	0.08	0.26

To further explore the relationships between the 10 CSW regions and the North Atlantic Ocean, North Pacific Ocean, and global oceans, trends for these regions and oceans for the period of 1970-2022 were calculated and are listed in Table 4. It is evident that both the North Atlantic (0.21°C/decade; p<0.05) and North Pacific (0.16°C/decade; p<0.05) exhibit stronger warming trends compared to the global oceans (0.10°C/decade; p<0.05), with the North Atlantic warming at a faster rate than the North Pacific during the last five decades. The BCS demonstrates the same warming trend as the North Pacific, while the SBS maintains a warming trend consistent with that of the global oceans. Among the 8 regions in the North Atlantic, there are notable variations in their warming trends. From the NNS to BB (the northern portion of the ocean), the trends are smaller than those of the North Atlantic Ocean.

Conversely, regions in southern Atlantic Canada exhibit trends higher than those of the North Atlantic, with the SS showing the strongest warming trend (0.38°C/decade) among all the regions. Note that all these trends are statistically significant (p values <0.05).

Table 4. Trends for the period of 1970-2022 for the global oceans, North Atlantic, North Pacific and the 10 sub-regions. Unit: ${}^{\circ}$ C/decade (HadISST)

	Global oceans: 0.10											
North Atlantic: 0.21 North Pacific: 0.16												
GoM	SS	GSL	SNS	S NNS LS HB BB		BCS	SBS					
0.28	0.38	0.32	0.24	0.21	0.16	0.15	0.12	0.16	0.10			

3.2 Historical SST changes

This section focuses on the changes in sea surface temperature (SST) within the 10 CSW regions with the average of the period 2012-2022 referenced to a 26-year climatology (1955-1980). Figure 4 depicts the spatial and geographical variations in SST changes within the Canadian Shelf Waters (CSW), with larger changes observed in the south and smaller changes in the north. The SST changes in these regions are visually represented in the bar plot of Figure 4 and are detailed in Table 5.

The SS exhibits the largest change among the 10 regions, with a rise of nearly 2°C. Conversely, the BB experiences the smallest change, at 0.4°C. The SS, GoM, GSL, and SNS regions all have SST increases exceeding 1°C. The influence of the cold Labrador Current, Western Greenland Current, and cold flows originating from the mostly ice-covered Arctic Ocean significantly impacts regions such as the BB, HB, LS, and the NNS. These regions experience reduced SST changes, often substantially smaller than 1°C, due to the influx of sea ice and cold water.

It is not surprising that the SBS shows only a modest SST change of approximately 0.5°C given its Arctic location which is covered by sea ice for many months of the year. The BCS demonstrates an SST change falling between that of the LS and NNS, approximately 0.7°C.

In an attempt to ground truth the changes in the CSW regions, the HadISST-derived results are compared to observation from DFO long-term monitoring stations. On the east coast, stations P5, S2, and S27 are used, while a composite time series from the British Columbia Shore Station Oceanographic Program is used for the west coast. The SST change in GoM is well represented by P5 (1.7°C vs 1.8°C, Table 5) while SST data from Station S2 underestimates the broader change on the SS (1.1°C vs 2.1°C).

The data for the Station S27 are for the whole water column from 0 m to 176 m, which explain why the S27 data significantly underestimates the SST change in NNS (0.2° C vs 0.9° C). For the west coast, the estimate of the changes in SST in the BCS is very similar to the change in SST by lighthouse stations (0.7° C vs 0.8° C).

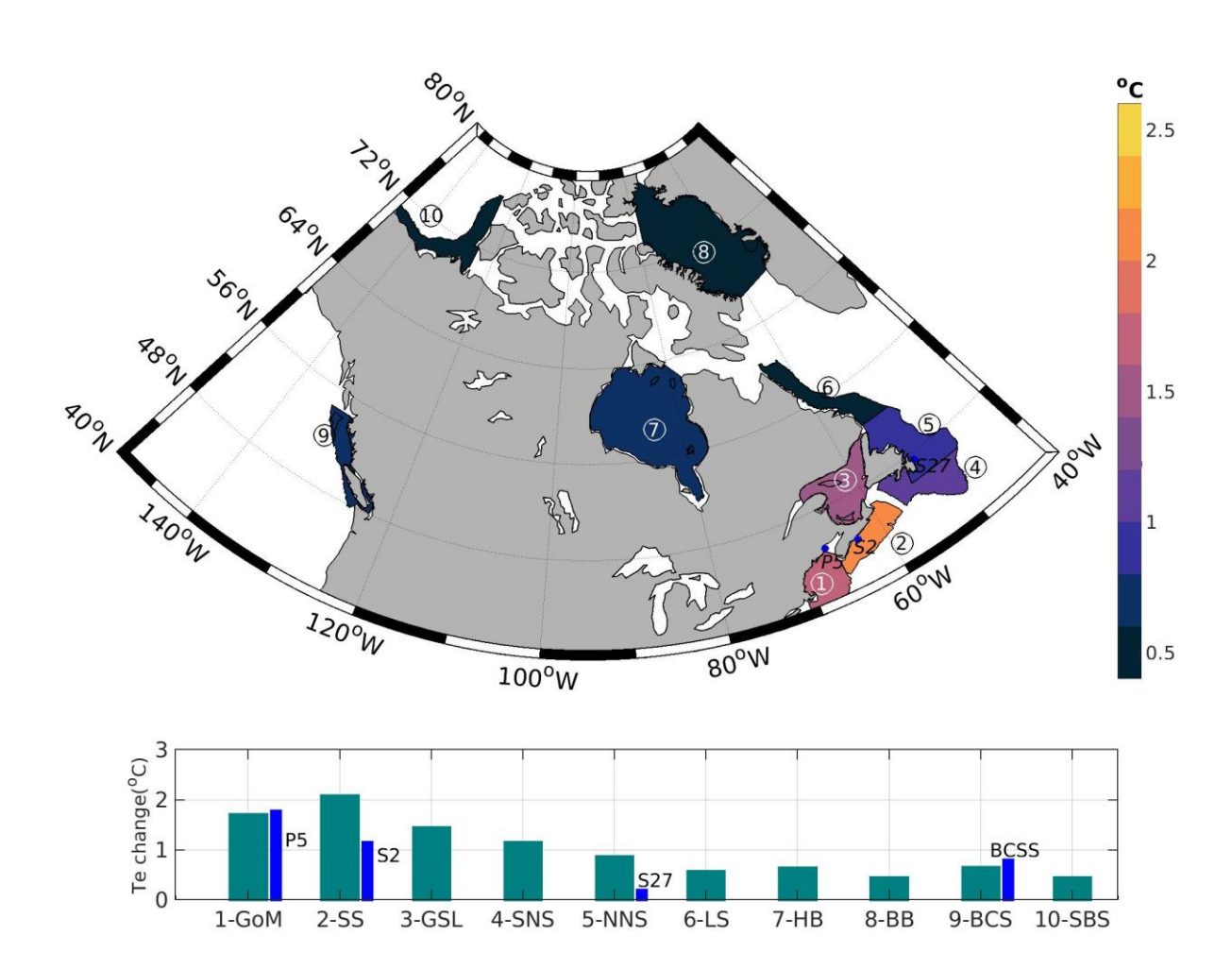


Figure 4: Map of the SST changes between 2012-2022 and 1955-1980 from HadISST for the 10 regions – annual means

Table 5. SST changes between 2012-2022 and 1955-1980 (°C) from HadISST – annual means

Regions	GoM/P5	SS/S2	GSL	SNS	NNS/S27	LS	HB	BB	BCS/BCSS	SBS
										Ì

(ΔT)	1.7/1.8	2.1/1.1	1.4	1.2	0.9/0.2	0.6	0.6	0.4	0.7/0.8	0.5

In the summer period (Jul-Sep, JAS), the combination of increased solar radiation, a shallower mixed layer, reduced heat loss, sea ice retreat and other potential feedback mechanisms can lead to more pronounced changes in SST trends compared to annual mean SST. A summary of the summer SST changes in summer is presented in Figure 5. Not surprisingly, the SST changes in the summertime in all the 10 sub-regions are consistently higher than the changes in the annual means (Table 6 vs Table 5). In terms of differences relative to the annual means, the GoM and BCS summer values have the smallest difference of 0.1 °C among the 10 regions. The HB shows the largest difference of 1.4 °C. All other regions have the SST differences between 0.5 to 0.8 °C.

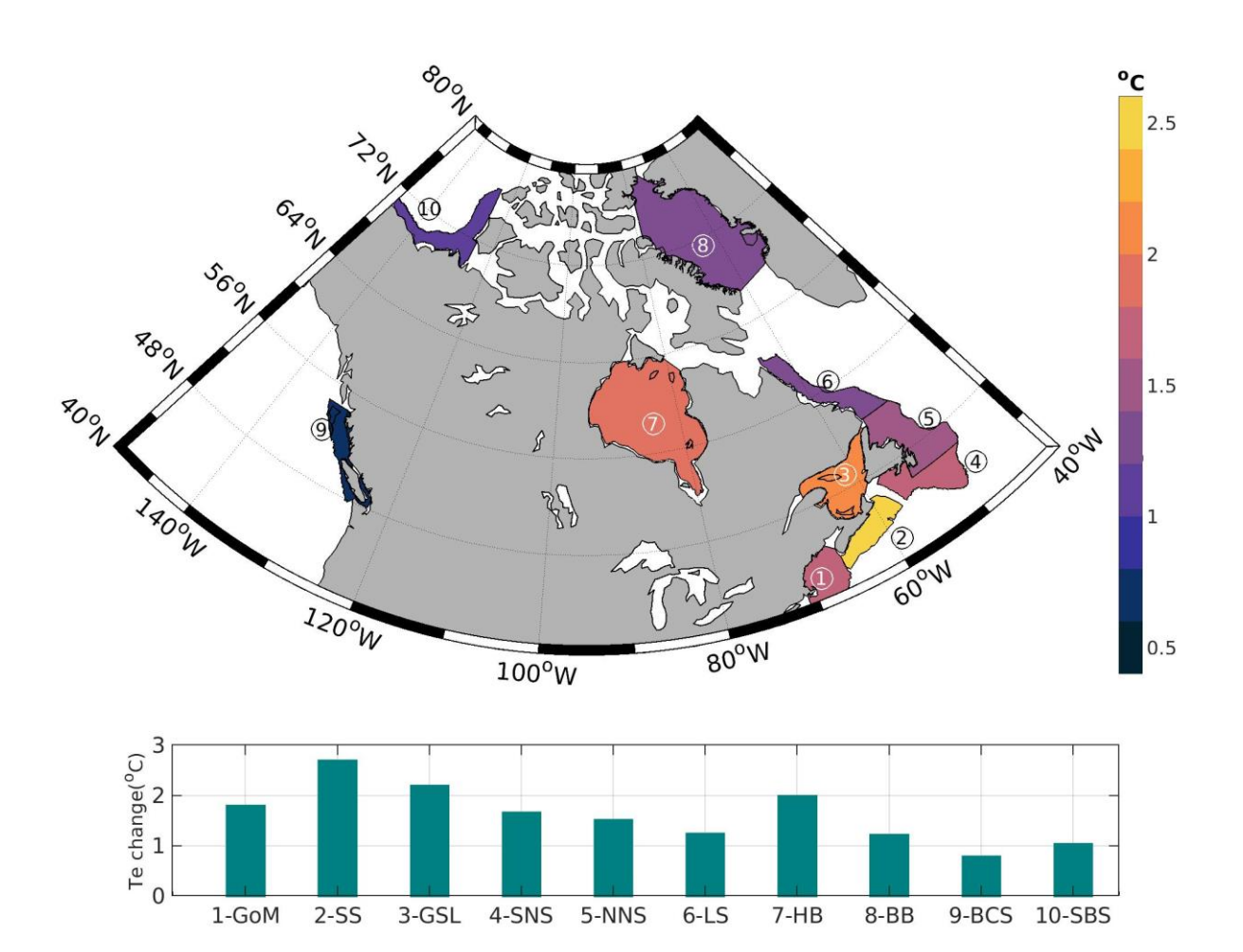


Figure 5: Map of the SST changes between 2012-2022 and 1955-1980 from HadISST for the 10 regions – summer (JAS) means

Table 6. SST changes between 2012-2022 and 1955-1980 (°C) – summer (JAS) means

regions	GoM	SS	GSL	SNS	NNS	LS	НВ	ВВ	BCS	SBS
(ΔT)	1.8	2.7	2.2	1.7	1.5	1.2	2.0	1.2	0.8	1.0

3.3 Projected SST changes

This study also evaluated the performance of the 22-member CMIP6 ensemble annual SST means for the 10 CSW regions by comparing temperature differences between 1990-2014 and 1955-1980, with results outlined in the appendix (Table A1). This analysis suggests that for the majority of the 10 CSW region CMIP6 model solutions tend to overestimate changes. However, overall, the changes from HadISST and those from CMIP6 models agree with each other closely. It is notable that the CMIP6 ensemble underestimates the SST change in the Scotian Shelf (SS) by 0.3°C, marking the largest difference between the HadISST and CMIP6 estimates of SST changes among the 10 regions.

Projected changes in SST in the defined CSW regions will be presented in the section for the future period of 2040-2059 referenced to the historic period of 1990-2014, with both derived from the ensemble CMIP6 outputs. While this report focuses on the future period of 2040-2059, there is similar analyses for the period of 2080-2099 provided in the Appendix. Annual mean SST changes are calculated for the 10 regions across all four Shared Socioeconomic Pathways (SSPs) and presented in the bar plot at the bottom of Figure 6. The map plot in Figure 6 visually presents the results of SST change based on the

scenario SSP2-4.5. The standard deviations presented in the bar plot in Figure 6 are calculated based on the data from the 22 CMIP6 models, and the values can be found in Table 7.

A comparison of Figure 6 to Figure 4 demonstrates that there is general consistency in the spatial distribution of projected and historical SST changes, albeit with a few notable differences. Firstly, the future SST change GSL now shows the largest SST change among the 10 regions, unlike the SS in Figure 4. Secondly, the SBS is projected to experience a stronger change than both BB and the LS while the BCS is expected to undergo a greater change than the NNS. Similar patterns are observed in the other three SSP scenarios. These findings highlight the importance of considering multiple scenarios when assessing future SST changes in the CSW.

As expected, the SST changes across the four SSPs from SSP1-2.6 to SSP5-8.5 exhibit a corresponding response to increasing greenhouse gas emissions, with higher emissions leading to greater SST changes (as depicted in the bar plot of Figure 6). Seven of the 10 regions, excluding the LS, BB, and SBS, experience SST increases above 1°C across all four scenarios by the mid-21st century (2040-2059). Regions such as the GoM, SS, GSL, and SNS exhibit temperature increases exceeding 1.5°C across all four SSPs. Moreover, these regions demonstrate increases surpassing 2°C, albeit remaining below 2.5°C under SSP5-8.5. The BB is the only region with SST increases below 1°C under all four climate scenarios due to the continued role of sea ice limiting SST increase in this region. It is notable that SST increases in the BCS region are similar under the SSP1-2.6, SSP2-4.5, and SSP3-7.0 scenarios, suggesting that there are complex mechanisms driving changes in the SST in this region. It is important to note that the CMIP6 model spread, as reflected in the standard deviations computed for each region, is large and, therefore, for any given scenario many of the regional means are not statistically different from each other. Hence, some caution is warranted in comparing these regional changes.

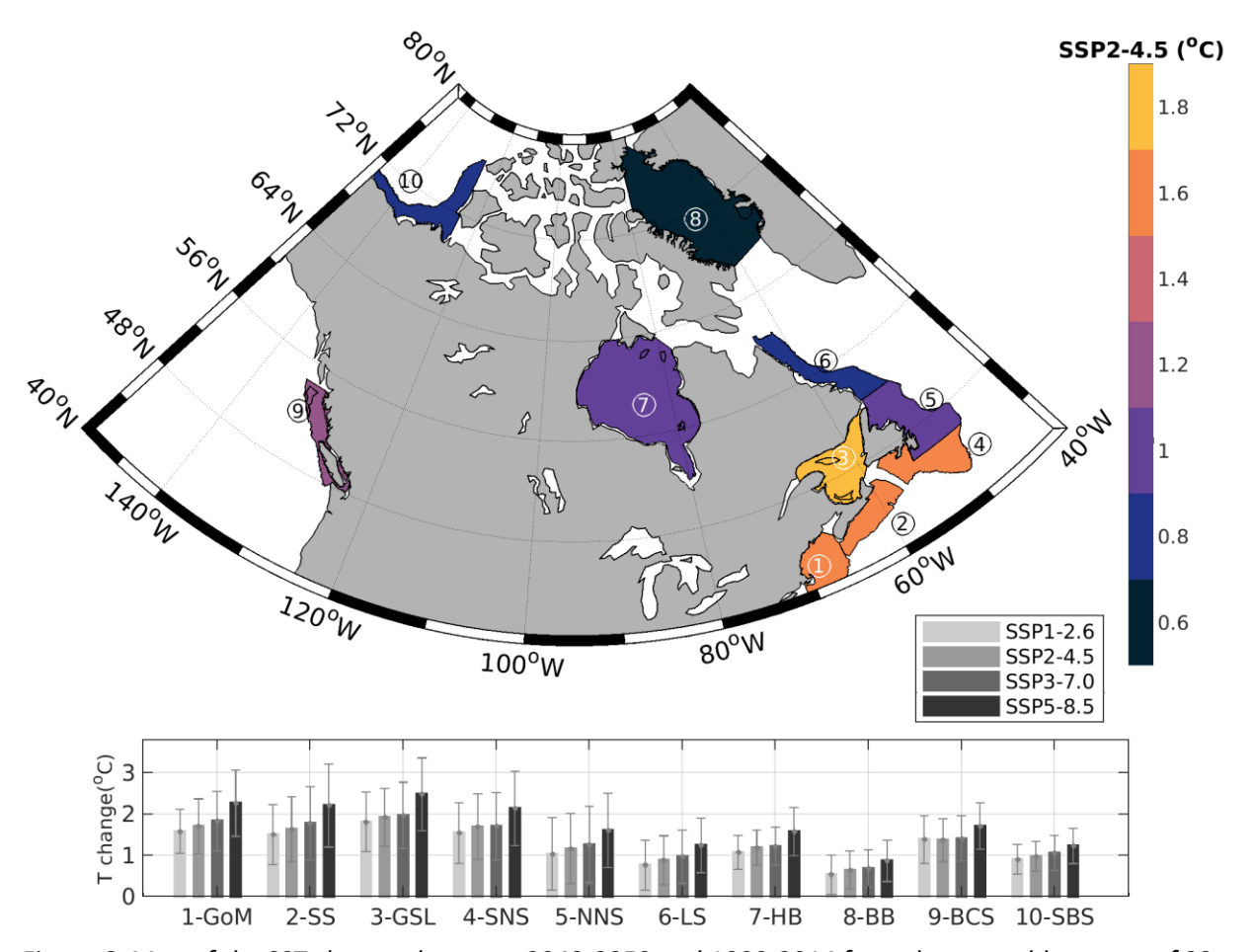


Figure 6: Map of the SST changes between 2040-2059 and 1990-2014 from the ensemble means of 22 CMIP6 models for the 10 regions — annual means. Note: the whiskers in the bar plot represent the standard deviations calculated based on the 22 models' results.

Table 7: SST changes between 2040-2059 and 1990-2014 for all the SSPs from the ensemble means of the CMIP6 models ($^{\circ}$ C)

	GoM	SS	GSL	SNS	NNS	LS	НВ	BB	BCS	SBS
SSP1-2.6	1.6±0.5	1.5±0.7	1.8±0.7	1.5±0.7	1.0±0.9	0.8±0.6	1.1±0.4	0.5±0.5	1.4±0.6	0.9±0.4
SSP2-4.5	1.7±0.7	1.6±0.8	1.9±0.7	1.7±0.8	1.2±0.8	0.9±0.6	1.2±0.4	0.7±0.5	1.4±0.5	1.0±0.4
SSP3-7.0	1.8±0.7	1.8±0.9	2.0±0.8	1.7±0.8	1.3±0.9	1.0±0.6	1.2±0.5	0.7±0.5	1.4±0.5	1.0±0.4
SSP5-8.5	2.3±0.8	2.2±1.0	2.5±0.9	2.1±0.9	1.6±0.9	1.2±0.7	1.6±0.6	0.9±0.5	1.7±0.6	1.2±0.4

The projected SST changes for the summer (JAS) are presented in Figure 7 and Table 8 with the standard deviations calculated based on the ensemble results from the 22 CMIP6 models. It is evident that the projected SST changes in summer are higher than the annual means in all the 10 regions (Table 8 vs Table 7). In the summer period, the SBS has the largest SST increase between the four scenarios (2.4 °C to 3.1 °C from SSP1-2.6 to SSP5-8.5), while the HB region has a slightly lower difference (2.1 °C to 3.0 °C from SSP1-2.6 to SSP5-8.5). The GSL, HB and SBS are all projected to have SST increase above 2.0 °C under the four climate scenarios. The SSP5-8.5 scenario projects all the 10 subregions to have SST increases of above 2.0 °C, with HB and SBS being above 3.0 °C. For the SSP1-2.6 scenario, only GSL, HB and SBS are projected to have SST increases above 2.0 °C, while the SNS region also exceeds the 2.0 °C threshold under SSP2-4.5.

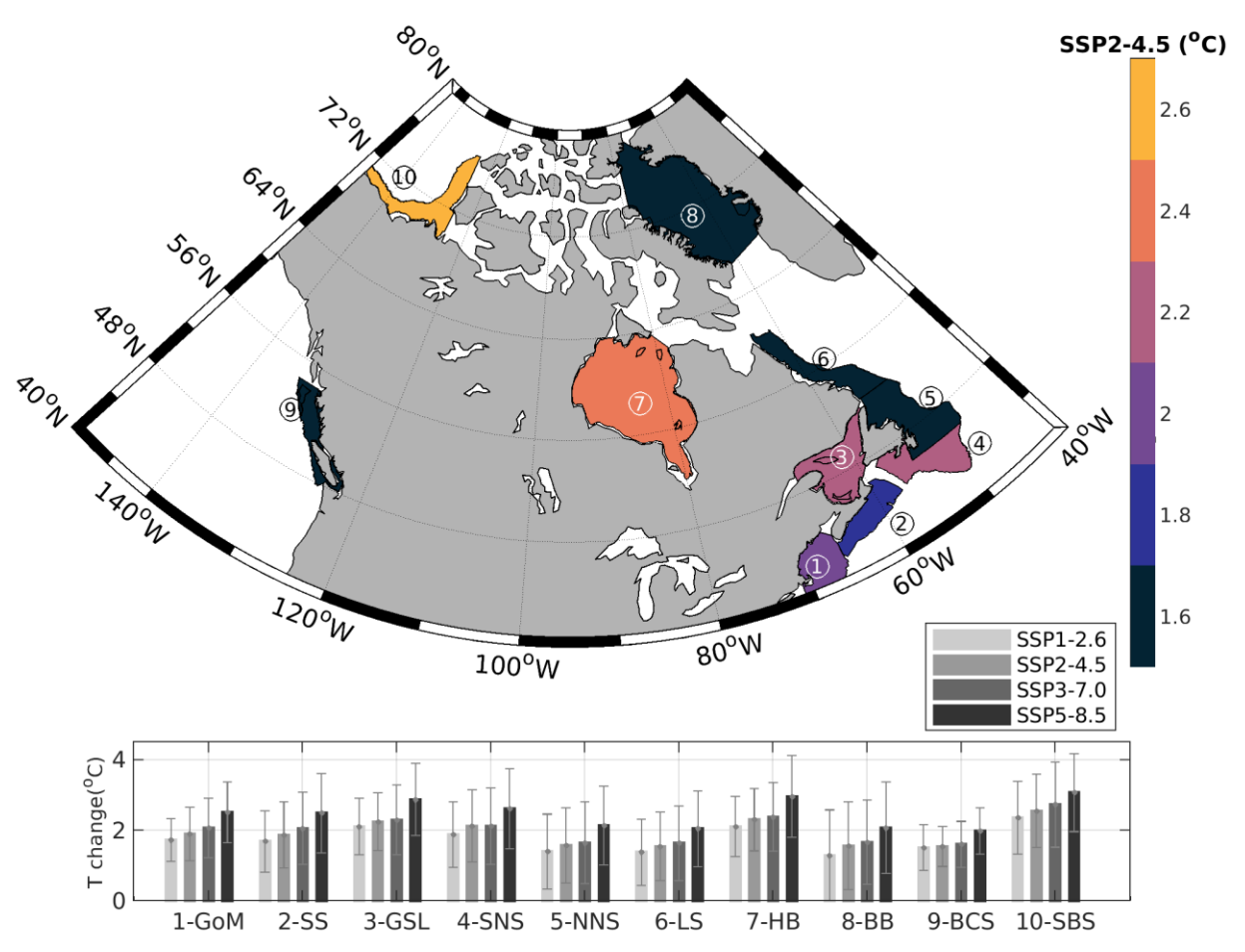


Figure 7: Map of the SST changes between 2040-2059 and 1990-2014 from the ensemble means of 22 CMIP6 models for the 10 regions – summer (JAS) means. Note: the whiskers in the bar plot represent the standard deviations calculated based on the 22 models' results.

Table 8: SST changes between 2040-2059 and 1990-2014 for all the SSPs from the ensemble summer(JAS) means of the CMIP6 models ($^{\circ}$ C)

	GoM	SS	GSL	SNS	NNS	LS	НВ	ВВ	BCS	SBS
SSP1-2.6	1.7±0.6	1.7±0.9	2.1±0.8	1.9±0.9	1.4±1.1	1.4±0.9	2.1±0.9	1.3±1.3	1.5±0.6	2.4±1.0
SSP2-4.5	1.9±0.8	1.9±0.9	2.2±0.8	2.1±1.0	1.6±1.1	1.6±1.0	2.3±0.9	1.6±1.3	1.5±0.6	2.6±1.0
SSP3-7.0	2.1±0.8	2.1±1.0	2.3±1.0	2.1±1.1	1.7±1.2	1.6±1.1	2.4±1.0	1.7±1.2	1.6±0.7	2.7±1.2
SSP5-8.5	2.5±0.9	2.5±1.1	2.9±1.0	2.6±1.1	2.1±1.1	2.0±1.1	3.0±1.2	2.1±1.3	2.0±0.7	3.1±1.1

The projected SST changes between 2080-2099 and 1990-2014 from the 22-member CMIP6 ensemble (annual and summer means) are shown in Appendix (Figure A1 and Table A2 for annual means; Figure A2 and Table A3 for summer means).

4. Discussion and conclusion

This study investigated the SST changes both in the past and future within the Canadian Shelf Waters (CSW). The focus of this study is on the annual and summer (JAS) mean SST.

Both the North Atlantic Ocean and the North Pacific Ocean exhibit multi-decadal variations, as depicted in Figure 1, and show warming trends from 1950-2022. In contrast, global oceans display less prominent multi-decadal variations, with a more continuous warming trend observed, as expected from our understanding of internal climate variability (Hawkins and Sutton, 2009, Deser et al, 2012, 2014). Variations in the global oceans predominantly occur on decadal or shorter timescales. The multi-decadal variability of the North Atlantic and North Pacific Oceans poses challenges in discerning warming trends over such periods, with these variations potentially representing natural rather than anthropogenic influences. Among the 10 CSW regions, the Gulf of St. Lawrence demonstrates a more consistent response to the entire North Atlantic Ocean, while most shelf regions in the North Atlantic better represent their oceanic counterpart compared to the British Columbia Shelf (BCS) for the North Pacific Ocean. This suggests differing responses of the CSW to their respective adjacent oceans, implying variations in driving dynamics between the two oceans. The winter convection in the Labrador Sea, a significant phenomenon in the North Atlantic Ocean (Wang et al., 2016, 2019; Yashayaev and Loder, 2016), is not observed in the North Pacific Ocean. Previous studies have shown that large-scale

variations in SST are only partially reflected in local areas, emphasizing the complex dynamics at play (Loder and Wang, 2015).

This study reveals that SST variations between 30°N and 60°N (subtropical and subpolar) in the North Atlantic Ocean effectively capture the large-scale SST variability characterized by the Atlantic Multi-decadal Oscillation (AMO). Conversely, in the North Pacific Ocean over the same latitudinal range, the Pacific Decadal Oscillation (PDO) cannot be adequately represented by the SST variations. This suggests that basin-scale SST changes in the North Pacific Ocean encompass a larger spatial coverage and more complex spatial distribution compared to those in the North Atlantic Ocean. Furthermore, we observed that SST variations in the Canadian Shelf Waters (CSW) within the North Atlantic Ocean exhibit stronger correlations to the defined North Atlantic Ocean than with the AMO (Tables 2 and 3, non-detrended). Conversely, CSW SST variations in the North Pacific Ocean are more closely linked with the PDO than with the SST of the defined North Pacific Ocean (Tables 2 and 3).

Historical SST analysis (1950-2022) across the global ocean, the North Atlantic Ocean, the North Pacific Ocean, and the 10 regions of the CSW reveals larger warming trends (annual means) in both the North Atlantic and North Pacific compared to the global oceans (Table 4). In the North Atlantic Ocean, the northern portion of the CSW (from NNS to BB) exhibits less warming than the broader North Atlantic Ocean, while the southern portion demonstrates more warming. Specifically, there's a decreasing tendency for the warming from south to north in the North Atlantic Ocean (from SS to BB), with the exception of the Gulf of Maine (GoM), which shows a smaller increase than that of the Scotian Shelf (SS). The Scotian Shelf stands out with the strongest warming among all CSW regions. Additionally, the warming in the British Columbia Shelf (BCS) is similar to that of the North Pacific Ocean, while the southern Beaufort Sea has the smallest warming trend, consistent with the trend observed in the global oceans.

The Gulf of Maine, Scotian Shelf, Gulf of St. Lawrence, and Southern Newfoundland Shelf emerge as areas with the largest SST historical and future increases (annual means) among all CSW regions. This strong warming is evident in both the past SST product from HadlSST (Figure 4) and the future ensemble means from CMIP6 models (Figure 6). These regions lie in the confluence zone of the cold southward-flowing Labrador Current and the warm northeastward-flowing Gulf Stream (Loder et al., 1998). Recent studies (Brickman et al., 2018; Seidov et al., 2021; Townsend et al., 2023) suggest that recent decadal-scale warming in this area may be partially attributed to changes in the Gulf Stream position and behaviour, with reports of weakening in the Gulf Stream (Wang et al., 2022) and indications of continued weakening.

The discrepancy between the observed strongest SST increase on the Scotian Shelf, as indicated by the HadlSST product, and the projected strongest increase in the Gulf of St. Lawrence from CMIP6 models can likely be attributed to the tendency of CMIP6 models to underestimate SST changes in the Scotian Shelf region (Table A1). This discrepancy underscores the importance of model resolution in accurately capturing the interaction between the Labrador Current and the Gulf Stream at the tip of Grand Banks, as highlighted in studies such as Brickman et al. (2018). Eddy blocking effects in this area are believed to be the primary cause of recent warming events on the Scotian Shelf (Brickman et al., 2018). However, the coarse resolution of CMIP6 models may fail to resolve these dynamics adequately, leading to the underestimation of strong SST increases in this region. This suggests that increasing model resolutions is necessary for better projections, particularly for the Scotian Shelf region (Saba et al., 2016).

Holdsworth et al. (2021) employed a high-resolution (1/36°) Northeast Pacific Model for climate downscaling and found British Columbia Shelf (BCS) SST increases ranging from 1.8–2.4°C for the RCP4.5 and RCP8.5 scenarios by mid-century (2046–2065 with a reference period of 1986–2005). In

comparison, the analysis in this study of the 22-member CMIP6 ensemble projects temperature increases ranging from 1.5°C for SSP2-4.5 to 1.9°C for SSP5-8.5 by mid-century (2040-2059 with a reference period of 1990-2014). It's important to note that Holdsworth et al. (2021) downscaled only one CMIP5 model, whereas our analysis is based on ensemble means over 22 CMIP6 models. Despite this difference, it is evident that the SST changes in our analysis align closely with their projections, albeit with slightly lower values. The differences in the future averaging period and the reference periods of the two studies could account for these variances in values. These findings suggest that while high-resolution models can provide detailed projections, low-resolution models may still offer reliable projections for certain regions of the Canadian Shelf Waters (CSW).

The Gulf of Maine and British Columbia Shelf exhibit the smallest differences in projected changes between summer means and annual means for both the historical period and for all four future scenarios; these are regions that do not form sea ice in the winter period. The Southern Beaufort Sea show the most significant differences between summer mean and annual mean sea surface temperatures followed by the Hudson Bay, both of which are ice-covered for a larger portion of each year. Historically, the Hudson Bay has experienced the greatest variation between summer and annual mean SSTs as recorded by the HadlSST. As Arctic air temperatures rise due to global warming, leading to reduced ice cover, the surface waters of the Arctic Ocean become increasingly influenced by atmospheric warming. This could explain why the Southern Beaufort Sea experiences the most pronounced projected changes between summer and annual means. The Southern Newfoundland Shelf and Northern Newfoundland Shelf show identical SST variations between summer and annual means. Interestingly, a gradual increase in the difference between these two measures can be observed from the Scotian Shelf in the south to the Hudson Bay in the north, suggesting the influence of latitude on summer-to-annual SST changes.

Tables 7 and 8 demonstrate large spreads of the SST changes in each climate scenario (STD), as is consistent with previous studies. The investigation of the historical changes in these 10 regions (Table 6) shows that the changes among these regions are generally small, though differences are clear. We suggest that changes in the SST in the CSW regions at long-time scales (20 years in this case) are dominated by the changes in the atmosphere and oceans at the large scales, but we must also stress that the coarse resolution of the CMIP6 models could also be a factor in the relatively small changes estimated among the four climate scenarios and the 10 regions.

Acknowledgements

This study is supported by the CSRF project - CC-22-05-01. Frederic Cyr provided the station S27 data.

Brendan DeTracey processed the CMIP6 data. Colleagues, Stephanie Clay and Li Zhai reviewed the report and provided helpful comments.

References

Baye et al., (2019). Modelling Atlantic mackerel spawning habitat suitability and its future distribution in the Northwest Atlantic. Fisheries Oceanography.

Beazley, L., Kenchington, E., Murillo, F.J., Brickman, D. and others (2021). Climate change winner in the deep sea? Predicting the impacts of climate change on the distribution of the glass sponge Vazella pourtalesii. Mar Ecol Prog Ser 657:1-23. https://doi.org/10.3354/meps13566

Beazley, L., Wang, Z., Kenchington, E., Yashayaev, I. and others (2021). Predicted distribution of the glass sponge Vazella pourtalesi on the Scotian Shelf and its persistence in the face of climatic variability. PLoS One, 13 (2018), p. e0205505, 10.1371/journal.pone.0205505

Brickman, D., Hebert, D., Wang, Z., (2018). Mechanism for the recent ocean warming events on the Scotian Shelf of eastern Canada. Cont. Shelf Res. 156, 11-22 https://doi.org/10.1016/j.csr.2018.01.001.

Checkley, D.M. and Barth, J.A. (2009). Patterns and processes in the California Current System, Prog. Oceanography, 83, p 49-64. https://doi.org/10.1016/j.pocean.2009.07.028

Cummins, P. F., & Masson, D. (2014). Climatic variability and trends in the surface waters of coastal British Columbia. Progress in Oceanography, 120, 279–290.

https://doi.org/10.1016/j.pocean.2013.10.002

Cyr, F. and Galbraith, P. S. (2021). A climate index for the Newfoundland and Labrador shelf, Earth Syst. Sci. Data, 13, 1807–1828, https://doi.org/10.5194/essd-13-1807-2021.

Cyr, F., Lewis, K., Bélanger, D., Regular, P., Clay, S. and Devred, E. (2024). Physical controls and ecological implications of the timing of the spring phytoplankton bloom on the Newfoundland and Labrador shelf. Limnol. Oceanogr. Lett. https://doi.org/10.1002/lol2.10347

Deser, C., Knutti, R., Solomon, S., & Phillips, A. S. (2012). Communication of the role of natural variability in future North American climate. Nature Climate Change, 2(11), 775–779. https://doi.org/10.1038/nclimate1562

Deser, C., Phillips, A. S., Alexander, M. A., & Smoliak, B. V. (2014). Projecting North American Climate over the Next 50 Years: Uncertainty due to Internal Variability. Journal of Climate, 27(6), 2271–2296. https://doi.org/10.1175/JCLI-D-13-00451.1

Donnet, S., Chandler, P., & Cummins, P. (2023). Sea surface temperature and salinity along the B. C. coast in 2022. In: Boldt, J.L., Joyce, E., Tucker, S., and Gauthier, S. (Eds.). 2023. State of the physical, biological and selected fishery resources of Pacific Canadian marine ecosystems in 2022. Can. Tech. Rep. Fish. Aquat. Sci. 3542, viii + 312p.

Eyring, V. and Bony, S. and Meehl, G. A. and Senior, C. A. and Stevens, B. and Stouffer, R. J. and Taylor, K. E. (2016). Overview of the Coupled Model Intercomparison Project Phase 6 (CMIP6) experimental design and organization. Geosci. Model Dev., 9, 1937-1958, doi:10.5194/gmd-9-1937-2016

Greenan, B., Shackell, N., Ferguson, K., Greyson, P., Cogswell, A., Brickman, D., Wang, Z., Cook, A., Brennan, C., and Saba, V. (2019). Climate Change Vulnerability of American Lobster Fishing Communities in Atlantic Canada. Frontiers in Marine Science. https://doi.org/10.3389/fmars.2019.00579

Han, G., Ma, Z., Long, Z., Perrie, W., and Chassé, J. (2019). Climate Change on Newfoundland and Labrador Shelves: Results From a Regional Downscaled Ocean and Sea-Ice Model Under an A1B Forcing Scenario 2011–2069, Atmosphere-Ocean, 57:1, 3-17, DOI: 10.1080/07055900.2017.1417110

Hawkins, E., & Sutton, R. (2009). The Potential to Narrow Uncertainty in Regional Climate Predictions. Bulletin of the American Meteorological Society, 90(8), 1095–1108.

https://doi.org/10.1175/2009BAMS2607.1

Holdsworth, A. M., Zhai, L., Lu, Y., and Christian, J. R. (2021). Future changes in oceanography and biogeochemistry along the Canadian Pacificcontinental margin. Frontiers in Marine Science, 8, 602991. https://doi.org/10.3389/fmars.2021.602991

Huang, B., Liu, C., Banzon, V., Freeman, E., Graham, G., Hankins, B., Smith, T., and Zhang, H. (2021). Improvements of the Daily Optimum Interpolation Sea Surface Temperature (DOISST) Version 2.1. J. Climate, 34, 2923–2939, https://doi.org/10.1175/JCLI-D-20-0166.1.

Ishii, M., Shouji, A., Sugimoto, S., and Matsumoto, T. (2005). Objective analyses of sea-surface temperature and marine meteorological variables for the 20th century using COADS and the KOBE collection. International Journal of Climatology, 25, 865-869.

Kenchington, E., Wang, Z., Lirette, C., Murillo, F.J., Guijarro, J., Yashayaev, I., Maldonado, M. (2019).

Connectivity modelling of areas closed to protect vulnerable marine ecosystems in the northwest

Atlantic. Deep-Sea Res. https://doi.org/10.1016/j.dsr.2018.11.007

Larouche, P. and Galbraith, P.S. (2016). Canadian coastal seas and Great Lakes sea surface temperature climatology and recent trends. *Canadian Journal of Remote Sensing*, *42*(3), pp.243-258.

Le Corre, N., Pepin, P., Burmeister, A., Walkusz, W., Skanes, K., Wang, Z., Brickman, D. and Snelgrove. P.V.R. (2020). Larval connectivity of northern shrimp (Pandalus borealis) in the Northwest Atlantic. Canadian Journal of Fisheries and Aquatic Sciences. 77(8): 1332-1347. https://doi.org/10.1139/cjfas-2019-0454

Lehmann, N., Reed, D. C., Buchwald, C., Lavoie, D., Yeats, P. A., Mei, Z.-P., et al. (2023). Decadal variability in subsurface nutrient availability on the Scotian Shelf reflects changes in the Northwest Atlantic Ocean. Journal of Geophysical Research: Oceans, 128, e2023JC019928.

https://doi.org/10.1029/2023JC019928

Loder, J. W., Baaren, A., and Yashayaev, I. (2015). Climate comparisons and change projections for the northwest Atlantic from Six CMIP5 models. Atmosphere-Ocean, 53(5), 529–555.

https://doi.org/10.1080/07055900.2015.1087836

Loder, J. W., Petrie, B., and Gawarkiewicz, G. (1998). The coastal ocean off north-eastern North America: A large-scale view. In A. R. Robinson, & K. H. Brink (Eds.), The Sea 11 (pp. 105–133).

Loder, J. W. and Wang, Z. (2015). Trends and Variability of Sea Surface Temperature in the Northwest Atlantic from Three Historical Gridded Datasets, Atmosphere-Ocean, 53:5, 510-528, DOI: 10.1080/07055900.2015.1071237

Loder, J.W., Baaren, A., and Yashayaev, I. (2015). Climate Comparisons and Change Projections for the Northwest Atlantic from Six CMIP5 Models, Atmosphere-Ocean, 53:5, 529-555, DOI: 10.1080/07055900.2015.1087836.

Lowen, J. B., and DiBacco, C. (2017). Distributional changes in a guild of a non-indigenous tunicates in the NW Atlantic under high resolution climate scenarios. Mar. Ecol. Prog. Ser. **570**, 173–186.

Lyons, D., Lowen, B., Therriault, T., Brickman, D., Pena, A., Wang, Z., and DiBacco, C. (2019). Identifying Marine Invasion Hotspots Using Stacked Species Distribution Models.

Marsh, R., Petrie, B., Weidman, C.R., Dickson, R.R., Loder, J.W., Hannah, C.G., Frank, K. and Drinkwater, K. (1999). The 1882 tilefish kill — a cold event in shelf waters off the north-eastern United States?. Fisheries Oceanography, 8: 39-49. https://doi.org/10.1046/j.1365-2419.1999.00092.x

Meehl, G. A., Covey, C., Taylor, K. E., Delworth, T., Stouffer, R. J., Latif, M., McAvaney, B., and Mitchell, J. F. B. (2007). THE WCRP CMIP3 Multimodel Dataset: A New Era in Climate Change Research, B. Am. Meteorol. Soc., 88, 1383–1394.

O'Brien, J M., Stanley, R., Jeffery, N. W., Susan G.H., Claudio, D., and Wang, Z. (2022). Modeling Demersal Fish and Benthic Invertebrate Assemblages in Support of Marine Conservation Planning. Ecological Applications 32(3): e2546. https://doi.org/10.1002/eap.2546

Okey, T.A., Alidina, H.M., Lo, V. et al. Effects of climate change on Canada's Pacific marine ecosystems: a summary of scientific knowledge. Rev Fish Biol Fisheries 24, 519–559 (2014).

https://doi.org/10.1007/s11160-014-9342-1

Pereira, H., Picado, A., Sousa, M.C., Alvarez, I., Dias, J.M. (2024). Assessing CMIP6 models in simulating meteo-oceanographic variability on Spanish continental coasts, Ocean Modelling, Volume 190, https://doi.org/10.1016/j.ocemod.2024.102395.

Pratt, C., Denley, D., Metaxas, A. (2022). Ocean warming and multiple source populations increase the threat of an invasive bryozoan to kelp beds in the northwest Atlantic Ocean. Mar Ecol Prog Ser 695:65-81. https://doi.org/10.3354/meps14121

Purich, A., & England, M. H. (2021). Historical and future projected warming of Antarctic Shelf Bottom Water in CMIP6 models. Geophysical Research Letters, 48, e2021GL092752.

https://doi.org/10.1029/2021GL092752

Rayner, N. A., Parker, D. E., Horton, E. B., Folland, C. K., Alexander, L. V., Rowell, D. P., Kent, E. C., Kaplan, A. (2003). Global analyses of sea surface temperature, sea ice, and night marine air temperature since the late nineteenth century J. Geophys. Res. Vol. 108, No. D14, 4407 10.1029/2002JD002670

Ren, Q., Y. Kwon, J. Yang, R. X. Huang, Y. Li, and F. Wang, 2024: Substantial Warming of the Atlantic Ocean in CMIP6 Models. J. Climate, 37, 3073–3091, https://doi.org/10.1175/JCLI-D-23-0418.1.

Saba, V. S., et al. (2016), Enhanced warming of the Northwest Atlantic Ocean under climate change, J. Geophys. Res. Oceans, 121, 118–132, doi:10.1002/2015JC011346.

Seidov, D., Mishonov, A. and Parsons, R. (2021), Recent warming and decadal variability of Gulf of Maine and Slope Water. Limnol Oceanogr, 66: 3472-3488. https://doi.org/10.1002/lno.11892

Shackell, N., Ferguson, K., Heyer, C., Brickman, D., Wang, Z., and Ransier, K.(2019). Growing degree-day influences growth rate and length of maturity of Northwest Atlantic halibut (Hippoglossus hippoglussus L.) across the southern stock domain. Northw. Atl. Fish. Sci.

Smith, T.M., Reynolds, R.W., Peterson, T.C., & Lawrimore, L. (2008). Improvements to NOAA's historical merged land-ocean surface temperature analysis (1880-2006). Journal of Climate, 21, 2283-2296. doi:10.1175/2007JCLI2100.1

Stanley, R., DiBacco, C., Lowen, B., Beiko, R., Jeffery, N., Wyngaarden, M., Bentzen, P., Brickman, D., Benestan, L., Bernatchez, L., Johnson, C., Snelgrove, P., Wang, Z., Wringe, B., and Bradbury, I.(2018). A climate-associated multispecies cryptic cline in the northwest Atlantic. Science. Advances, 4, eaaq0929.

Stevenson, S., Huang, X., Zhao, Y., Di Lorenzo, E., Newman, M., van Roekel, L., et al. (2023). Ensemble spread behavior in coupled climate models: Insights from the Energy Exascale Earth System Model version 1 large ensemble. Journal of Advances in Modeling Earth Systems, 15, e2023MS003653. https://doi.org/10.1029/2023MS003653

Taylor, K. E., Stouffer, R. J., and Meehl G. A.(2012). An Overview of CMIP5 and the Experiment Design, B. Am. Meteorol. Soc., 93, 485–498.

Townsend, D. W., Pettigrew, N. R., Thomas, M. A., Moore, S. (2023). Warming waters of the Gulf of Maine: The role of Shelf, Slope and Gulf Stream Water masses, Progress in Oceanography, https://doi.org/10.1016/j.pocean.2023.103030.

Wang, S., Kenchington, E.L., Wang, Z. et al.(2020a). 3-D ocean particle tracking modeling reveals extensive vertical movement and downstream interdependence of closed areas in the northwest Atlantic. Sci Rep 10, 21421. https://doi.org/10.1038/s41598-020-76617-x

Wang, Z., Brickman, D., Greenan, B.J.W., Yashayaev, I. (2016). An abrupt shift in the Labrador Current System in relation to winter NAO events. J. Geophys. Res. Oceans 121, 5338–5349, https://doi.org/doi:10.1002/2016JC011721.

Wang, Z., Brickman, D., Greenan, B. (2019). Characteristic evolution of the Atlantic Meridional

Overturning Circulation from 1990 to 2015: An eddy-resolving ocean model study. Deep Sea Research

Part I 149 103056

Wang, Z., Brickman, D., Greenan, B., Christian, J., DeTracey, B., & Gilbert, D. (2024). Assessment of Ocean Temperature Trends for the Scotian Shelf and Gulf of Maine Using 22 CMIP6 Earth System Models, Atmosphere-Ocean, 62:1, 24-34, DOI: 10.1080/07055900.2023.2264832

Wang, Z., Horwitz, R., Bowlby, H.D., Ding, F., Joyce, W.N. (2020b) Changes in ocean conditions and hurricanes affect porbeagle Lamna nasus diving behavior. Mar Ecol Prog Ser 654:219-224. https://doi.org/10.3354/meps13503

Wang, Z., Lu, Y., Dupont, F., Loder, J., Hannah, C., and Wright, D. (2015), Variability of sea surface height and circulation in the North Atlantic: Forcing mechanisms and linkages, Progress in Oceanography. Doi: 10.1016/j.pocean.2013.11.004.

Wang, Z., Yang, J., Johnson, C., and DeTracey, B. (2022). Changes in deep ocean contribute to a "see-sawing" Gulf Stream path. Geophysical Research Letters, 49, e2022GL100937.

https://doi.org/10.1029/2022GL100937

Wassmann, P., Duarte, C.M., Agusti, S. and Sejr, M.K. (2011), Footprints of climate change in the Arctic marine ecosystem. Global Change Biology, 17: 1235-1249. https://doi.org/10.1111/j.1365-2486.2010.02311.x

Yashayaev, I., Loder, J.W. (2016). Recurrent replenishment of Labrador Sea Water and associated decadal-scale variability. J. Geophys. Res. Oceans 121, 8095–8114, https://doi.org/10.1002/2016JC012046.

Zhang, Q., Liu, B., Li, S. and Zhou, T., 2023. Understanding models' global sea surface temperature bias in mean state: from CMIP5 to CMIP6. Geophysical Research Letters, 50(4), p.e2022GL100888.

Appendix

Table A1. Mean SST for the 1955-1980 (T; HadISST) and SST changes between 1990-2014 and 1955-1980 (°C) from the HadISST and CMIP6

	GoM	SS	GSL	SNS	NNS	LS	НВ	BB	BCS	SBS
HadISST (T)	10.5	8.5	5.7	7.5	4.5	1.3	0.5	-0.4	10.1	-0.7
HadISST (ΔT)	0.7	1.0	0.7	0.6	0.5	0.4	0.4	0.2	0.2	0.2
CMIP6 (ΔT)	0.7	0.7	0.7	0.7	0.7	0.5	0.5	0.3	0.4	0.3

A summary of projected SST changes for the period 2080-2099 referenced to the historical period of 1990-2014 is provided here. These results are based on the ensemble means of 22 CMIP6 models for the 10 regions of the Canadian Shelf Waters.

2080-2099 vs 1990-2014

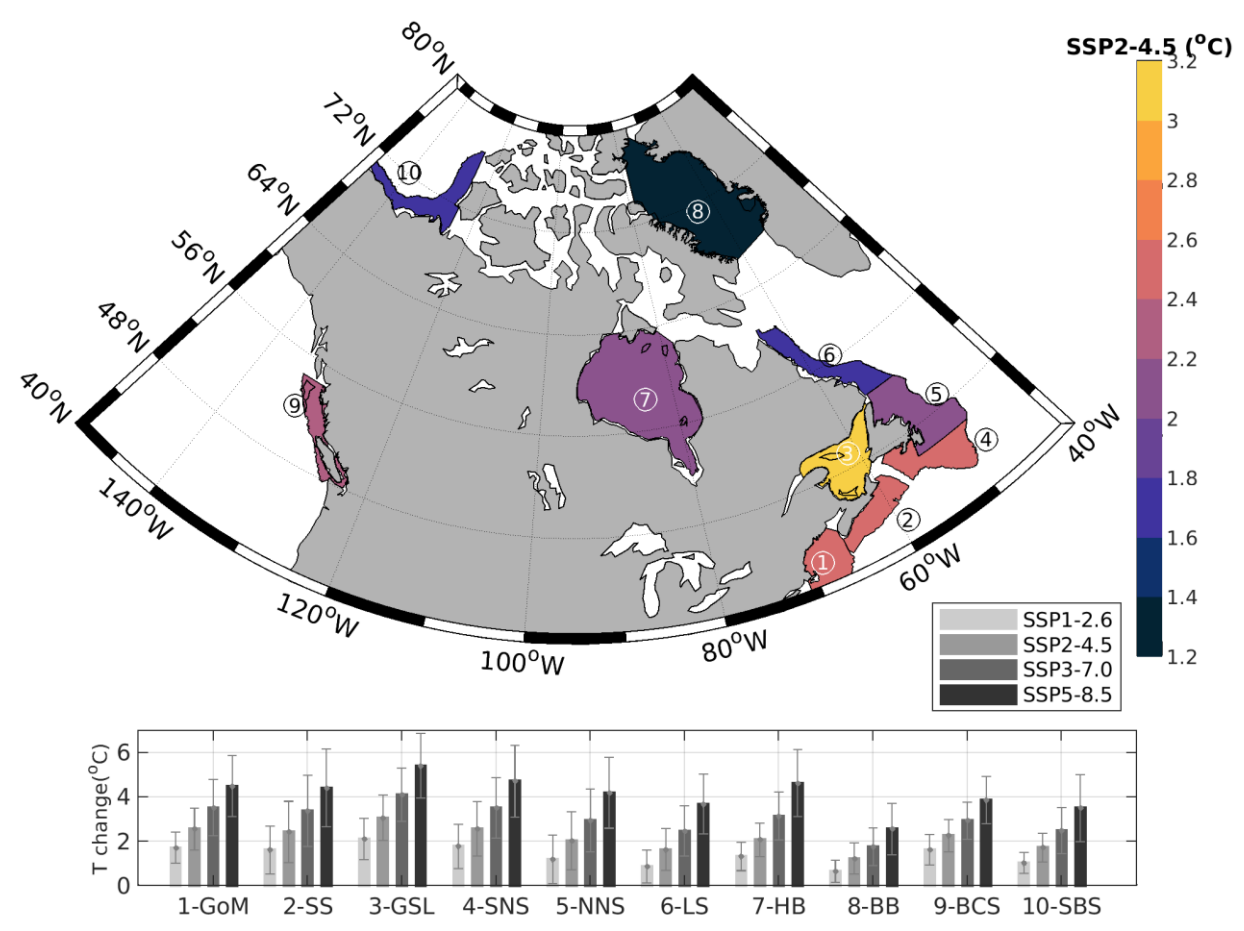


Figure A1: Map of the SST changes between 2080-2099 and 1990-2014 from the ensemble means of 22 CMIP6 models for the 10 regions – annual means. Note: the whiskers in the bar plot represent the standard deviations calculated based on the 22 models' results.

Table A2: SST changes between 2080-2099 and 1990-2014 for all the SSPs from the ensemble annual means of the CMIP6 models ($^{\circ}$ C)

	GoM	SS	GSL	SNS	NNS	LS	НВ	ВВ	BCS	SBS
SSP1-2.6	1.7±0.7	1.6±1.1	2.1±0.9	1.8±1.0	1.2±1.1	0.9±0.7	1.3±0.6	0.7±0.5	1.6±0.7	1.0±0.5
SSP2-4.5	2.6±0.9	2.4±1.4	3.1±1.0	2.6±1.2	2.0±1.3	1.6±0.9	2.1±0.8	1.2±0.7	2.3±0.7	1.7±0.7
SSP3-7.0	3.5±1.3	3.4±1.6	4.1±1.2	3.5±1.4	2.9±1.4	2.5±1.1	3.1±1.1	1.8±0.8	2.9±0.8	2.5±1.0
SSP5-8.5	4.5±1.4	4.4±1.8	5.4±1.4	4.7±1.6	4.2±1.6	3.7±1.3	4.6±1.5	2.6±1.2	3.9±1.1	3.5±1.5

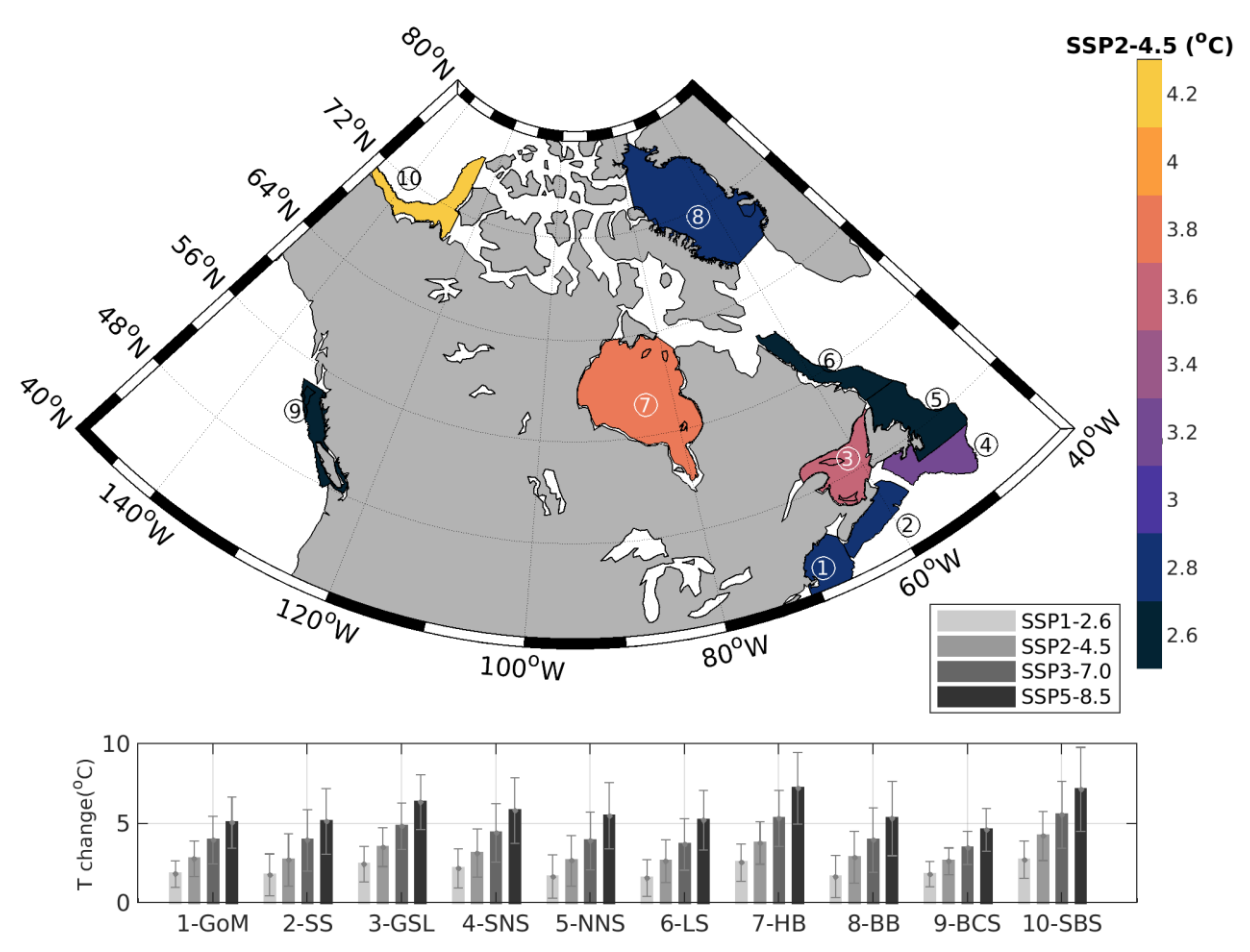


Figure A2: Map of the SST changes between 2080-2099 and 1990-2014 from the ensemble means of 22 CMIP6 models for the 10 regions – summer (JAS) means. Note: the whiskers in the bar plot represent the standard deviations calculated based on the 22 models' results.

Table A3: SST changes between 2080-2099 and 1990-2014 for all the SSPs from the ensemble summer (JAS) means of the CMIP6 models ($^{\circ}$ C)

	GoM	SS	GSL	SNS	NNS	LS	НВ	ВВ	BCS	SBS
SSP1-2.6	1.8±0.8	1.8±1.3	2.4±1.1	2.2±1.2	1.7±1.4	1.6±1.2	2.5±1.2	1.7±1.3	1.8±0.8	2.7±1.2
SSP2-4.5	2.8±1.1	2.7±1.6	3.5±1.2	3.1±1.5	2.7±1.6	2.6±1.4	3.8±1.3	2.9±1.6	2.6±0.8	4.2±1.5
SSP3-7.0	4.0±1.5	3.9±1.9	4.8±1.5	4.4±1.8	3.9±1.8	3.7±1.6	5.3±1.8	4.0±2.0	3.5±1.0	5.5±2.1
SSP5-8.5	5.1±1.6	5.1±2.1	6.3±1.7	5.8±2.1	5.5±2.1	5.2±1.9	7.2±2.2	5.3±2.3	4.6±1.3	7.2±2.6